Indian J Phys (May 2023) 97(6):1739–1747
https://doi.org/10.1007/s12648-022-02523-9

ORIGINAL PAPER

Role of S/Se replacement on the structure of $Ge_{20}Se_{80-x}S_x$ glasses

A F Elhady*, M Dongol, M S Ebied and S Mahmoud

Nano and Thin Film Lab. Physics Department, Faculty of Science, South Valley University, Qena 83523, Egypt

Received: 08 July 2022 / Accepted: 26 October 2022 / Published online: 19 November 2022

Abstract: The effect of S-content on the medium-and short-range order structure of $Ge_{20}Se_{80-x}S_x$ $(x = 0, 15, 30at\%)$, has been investigated by using high-energy X-ray diffraction. Medium-range order changes, as illustrated by the parameters of the first sharp diffraction peak, were discussed in the light of the microcrystalline model. The short-range order parameters have been obtained by the analysis of the first two peaks in the curve of the total radial distribution function. The current results indicate that S-atoms enter the host network of the stiffness composition ($Ge_{20}Se_{80}$) as compensation of Se-atoms.

Keywords: Chalcogenides glasses; Glassy Ge-Se-S system; High energy X-ray diffraction; Medium range order; Short range order; Chemically ordered network

1. Introduction

In contrast to oxide glasses, chalcogenide glasses have semiconductor-type band gap, high refractive index, large third-order nonlinearity, and photosensitivity whilst being free of absorption across the whole of the near-and mid-infrared [1–3]. Such properties enabled many chalcogenide–based applications to be developed in divers fields including, photonic, medicine, military, and environmental sensing, [4, 5]. In addition, chalcogenide glasses seem to be one of most promising materials for catalysts and anticorrosion media [6, 7]. Consequently, understanding the short (SRO) and medium-range order (MRO) structure of these chalcogenide glasses is important to build predictive models of structure–property relationships [8].

Owing to its technological applications, the structure of the glassy Ge_xSe_{1-x} system has been extensively studied during the past decades [8–17]. Within the glass forming region $(x<0.43)$[18], the structure of these glasses is best described in terms of a chemically ordered network (CON) which depend on heteropolar bonds. The Ge atoms are covalently bonded to four Se atoms constituting $GeSe_4$ tetrahedra, while Se atoms coordinated with two Ge or Se atoms, depending on the concentration x.

Of all the different compositions of Ge_xSe_{1-x}, the composition $Ge_{20}Se_{80}$ acquires a special interest. According to mean-field constraint-counting theory [19, 20], the composition $Ge_{20}Se_{80}$ is considered as a milestone. The network in the range $x<20$ is elastic "floppy" or underconstrained, and in the range $x > 20$ it becomes "stressed-rigid" or over-constrained. The network of the composition $Ge_{20}Se_{80}$ is rigid or isostatic. The number of constraints per atom at this composition equals the degree of freedom. So, this composition constitutes a "stiffness" threshold between these excessive situations. Numerous experiments have been performed to show this threshold on the physical properties, various properties have shown extrema at this composition. Thermal expansion, isothermal compressibility, and macroscopic density, these properties show minimization at $x = 20$ [21, 22]. Also, valance band and conduction band photoemission spectral exhibit a special character in this composition [23]. Furthermore, this composition shows a maximum in the pressure transition at which the semiconducting network changes into a metallic crystalline phase [24 and refs. therein].

Considerable effort has been devoted to elucidate the effect of S/Se replacement on the structure of $Ge(Se_{1-x}S_x)_2$ [25–28]. The conclusion is that the structure is a combination of $GeSe_{(4-n)/2}S_{n/2}$ tetrahedra units (n=0-4). Rather less attention has been paid to studying the effect of S/Se replacement on the structure of $Ge_{20}Se_{80-x}S_x$ glasses. Results of Raman studies on bulk and thin films of this system have shown that, first: replacing Se with S leads to formation of both $GeSe_{(4-n)/2}S_{n/2}$ tetrahedra and Se_n chains, and second: The structure of $Ge_{20}Se_{80-x}S_x$ glasses

*Corresponding author, E-mail: abdelsalam.mohamed@sci.svu.edu.eg

is well described by chemically ordered network model [29, 30].

The purpose of the present work is to investigate short- and medium-range order structure of $Ge_{20}Se_{80-x}S_x$ (x = 0, 15, 30 at%), by using the method of high energy X-ray diffraction.

2. Experimental details

2.1. Sample preparation

Chemically pure Ge, S and Se (99.999%) are weighted according to the desired composition. Their mixture is immediately sealed in a silica glass ampule of 6 mm in external diameter and of 50 mm in length. Contents of the ampoule were sealed under vacuum of 10^{-4} torr. The ampoule is then heated in programmable electric furnace. The temperature is slowly raised up to 1273 K and the melt is kept at this temperature for 24 h. The ampoule was rotated during the melting at regular intervals to achieve homogenous mixing. The glassy samples of $Ge_{20}Se_{80-x}S_x$ of x = 0, 15 and 30 at% were produced by quenching the melt-in ice water mixture. The macroscopic densities of the studied system were determined at room temperature by the Archimedes method using distilled water as the immersion fluid.

2.2. High-energy X-ray diffraction

High-energy X-ray diffraction experiments were carried out, using X-rays of energy 86.6 keV ($\lambda = 0.1431\mathring{A}$) at room temperature, at the beamline ID-15-B ESRF Grenoble-France. This high energy provides diffraction data over higher values of $k(k = 4\pi\sin\theta/\lambda)$, leading to high resolution in real space [13].The prepared Samples were gently crushed into fine powder and then sealed in 1.2 mm diameter Kapton® capillaries and subjected to X-ray diffraction experiments in transmission geometry. A Perkin-Elmar large area 2D image plate detector was placed centered on and perpendicular to the incident beam 198 mm behind the sample. The sample-detector distance was calibrated using a NIST CeO_2 standard of known lattice parameter. Raw 2D diffraction pattern was corrected for background and then, 1D powder diffraction patterns were obtained by integrating around the Debye–Scherrer rings on the image plate images using the program Fit2D [31]. 1D background-corrected data were corrected for polarization, absorption, fluorescence, and Compton scattering [32, 33]. Then, the coherent intensity $I^{\mathrm{coh}}(k)$ was normalized to electron units per atom, $I_{\mathrm{eu}}^{\mathrm{coh}}(k)$, using Krogh-Moe – Norman method [34].The total structure factor, $S(k)$, is obtained from $I_{eu}^{coh}(k)$ as follows [35]:

$$S(k) = 1 + \frac{I_{\mathrm{eu}}^{\mathrm{coh}}(k) - \langle f^2(k)\rangle}{\langle f(k)\rangle^2} \quad (1)$$

where $\langle f\rangle = \sum_{i=1}^{m} x_i f_i(k)$ and $\langle f^2(k)\rangle = \sum_{i=1}^{m} x_i f_i^2(k)$, where x_i and $f_i(k)$ are, respectively, the atomic concentration and X-ray atomic scattering factor of the atom i. To get real-space structural information, the total radial distribution function, $T(r)$, has been obtained by Fourier transformation of the reciprocal space $S(k)$;

$$T(r) = 4\pi r\rho(r) = 4\pi r\rho_0 + \frac{2}{\pi}\int_0^{k_{\max}} k(S(k) - 1)\sin(kr)\mathrm{d}k \quad (2)$$

where r is the radial distance, $\rho(r)$ is the local atomic number density, and ρ_0 is the average atomic number density. These stages of data treatments were done with the aid of PDFgetX3 program [36]. The average coordination number, η, around any atom in a spherical shell between radii r_1 and r_2 is given by [37];

$$\eta = \int_{r_1}^{r_2} T(r)r\mathrm{d}r \quad (3)$$

3. Results and discussion

3.1. Reciprocal space properties

Figure 1 shows the measured $S(k)$ versus k for $Ge_{20}Se_{80-x}S_x$ glasses. If all corrections to the experimental data were known accurately and if the coherent and incoherent scattering factors were correct, $S(k)$ will oscillate smoothly along the value one at large k-values [25, 38]. This condition is satisfied, as shown in Fig. 1.

The effect of S/Se substitution on the atomic arrangement of reciprocal $k-$ space showed be evident in the characteristics of the first two peaks of $S(k)$. The first peak is called the first sharp diffraction peak (FSDP), observed at low $k-$ values ($0.8 < k < 1.6$ Å.$^{-1}$) in $S(k)$ curves of network-forming glasses and liquids. The second peak is called the Principle Peak (PP). The FSDP is more sharp comparing with the other peaks, and so it was named. Appearance of this peak is frequently considered as a signature for some kind of structure ordering at MRO [39, 40]. Origin of this peak- and hence the origin of MRO in non-crystalline materials is still controversy and, to some extent, vague subject. Various models have been proposed to account for the structural origin of the FSDP, [41–46]. Till now no theory can comprehensively and uniformly explain the origin of this feature. Sometimes, these comprehensive and unification were considered as a priority for

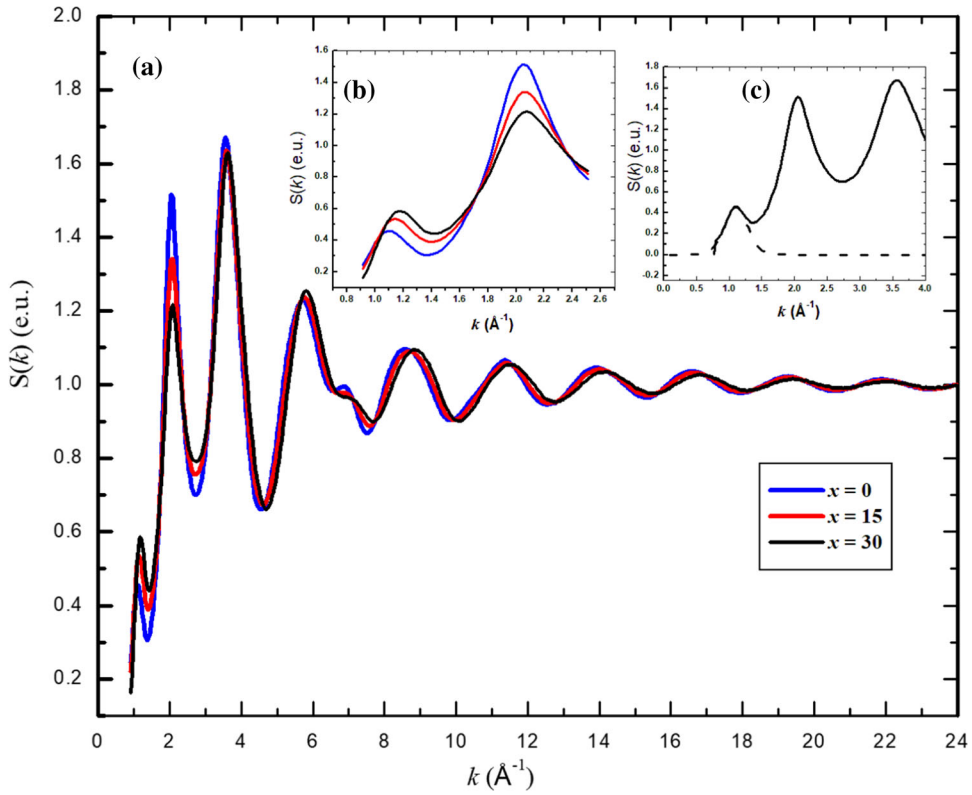

Fig. 1 (**a**) Total structure factor S(k) of $Ge_xSe_{80-x}S_x$ glasses. (**b**) The range of the first sharp diffraction peak (FSDP) and principle peak (PP). (**c**) Lorentzian fitting for FSDP of $Ge_xSe_{80-x}S_x$ glasses (dotted line)

accepting any theory or explanation articulate for MRO in no-crystalline materials [46, 47]. Parameters of the FSDP (position k_1, width Δk_1 and height I_1) are normally used as a criteria for the degree of MRO. In this context, MRO is measured by I_1, characteristic length $R = 2\pi/k_1$ and coherence length $L = 2\pi/\Delta k_1$ (where Δk_1 is the full-width at half-maximum of the FSDP) [39, 48]

The position of FSDP is often associated with oscillations in real space. These oscillations reflect some repetitive characteristic length R between the structural entities [39, 48]. Quantitively, it is possible to scale MRO using Debye equation [49]. The scattering intensity curves are deduced from a superposition of few Debye interference functions$\sin s/s$, where $s = k \cdot r$ with r is the period of the interference function. The maxima positions of the function $\sin s/s$ are given by the conditions$k \cdot r = \text{const.}$, with $const. = 7.728, 14.062, \ldots$. Now, if the FSDP is characterized by real distance (characteristic length) R corresponding to reciprocal space characteristic lengthk_1, then R may be estimated as $R \approx 2.5\pi/k_1$ [10, 50]. Similar relations were concluded by several author [51, 52]. Another estimation of the length$R$, based Bragg's law, leads to $R = 2\pi/k_1$. The first estimation is more probable because, from ono side, it's a direct result of Debye formula, and from the other side Bragg's law is applicable only when interference occurs over a large number of regularly spaced layers, while in the case of non-crystalline materials the number of such layers that may be considered as regularly spaced is not so large [50]. Nevertheless, the difference between the two methods is not so large, and we remarked that some authors used the first, and others used the second method freely. The correlation length,L, over which such quasi-periodic real-space density fluctuations are maintained, can be obtained from the full width at half maximum,Δk_1; $L = 2\pi/\Delta k_1$ [53].

Careful measurements of the FSDP had shown that it can be approximated well by a Lorentzian curve [54, 55]. Thus, We used Lorentzian approximation to evaluate the FSDP parameters. Figure (1c) shows the fitting results of $Ge_{20}Se_{80-x}S_x$ samples with$x = 0$. The characteristic length R and the correlation length L are calculated from the well-resolved FSDP for all samples and are given in Table 1.

Table 1, shows that increasing S content leads to slight growth in the intensityI_1. The same features was observed with S/Se replacement in $Ge(Se_{1-x}S_x)_2$, $Ge_3(Se_{1-x}S_x)_4$, $Ge(S)Se_2$ glasses [26, 44, 56]. On the other side, both k_1 and Δk_1 increase, which means decreasing both R and$L$, respectively. Conversely, increasing I_1 with increasing S-content is accompanied by decreasing in the principle peak (PP) position at$k_{PP} = 2.0\mathring{A}^{-1}$. The PP is associated with some extended-range order, which is related to a propagation of short-range ordering [12, 57]. Decreasing the intensity of PP would reflect some distortion on SRO with S/Se replacement. This will invstigate later. The opposite

Table 1 The position (k_1), the characteristic length R, the full width at half maximum Δk_1, the correlation length L and the height I_1 of the FSDP of $Ge_{20}Se_{80-x}S_x$ glasses

x	$k_1(\mathring{A}^{-1})$	R($\mathring{A}$)	$\Delta k_1(\mathring{A}^{-1})$	L($\mathring{A}$)	I_1
0	1.11 ± 0.02	5.67 ± 0.01	0.42 ± 0.06	15.14 ± 0.14	0.46 ± 0.04
	1.1 [14, 15, 67]				
15	1.15 ±0.01	5.48 ± 0.02	0.41 ± 0.01	15.33 ± 0.01	0.54 ± 0.02
30	1.17 ±0.05	5.38 ± 0.01	0.37 ± 0.01	17.15 ± 0.05	0.59 ± 0.01

behaviors of the FSDP and the PP are frequently observed with S/Se replacement [26, 56]. At first glance, the simultaneous increase in I_1 and Δk_1 might be a contradiction. To understand these features, we should have a look at the development of the MRO on Ge(S, Se) glasses. Analysis MRO of the Ge_xSe_{100-x} has been frequently considered [58–60]. According to the models which ascribe the FSDP to microcrystalline origin [41, 42, 62], the composition $Ge_{20}Se_{80}$ lies in the region of $15 < x < 0.33$ in which $GeSe_{4/2}$ units agglomerate into a mixture of corner-sharing (CS) and edge-sharing (ES) [10, 26], resulting in the layer-like structure similar to that of HT-$GeSe_2$ [62, 63]. Prevailing view is that the FSDP originated from correlations containing Ge atoms [26, 56, 58, 59]. The FSDP is also observed in the partial static-structure factor $S_{Ge-Se}(k)$ [64, 65]. In the floppy glass region of Ge_xSe_{1-x} glasses ($x \leq 20$ at%), the FSDP has two contributions of Ge–Ge and Se–Se correlations [66, 67]. In connection with MRO of Ge–S system, it was considered that the FSDP of GeS_2 is evoked by 2D-cluster structure due to rings [68] or layer-like outrigger rafts [69] as a remanence of the high temperature layer-like crystalline structure [70]. In GeS_2 the FSDP has a large contribution from Ge–Ge correlations [12]. Furthermore, the results of neutron diffraction show that the height of FSDP shows significant increasing with the transformation from $Ge_{20}Se_{80}$ to $Ge_{20}S_{80}$ [71]. In addition, it was shown that in chalcogen-rich system the tendency of Se atoms to form Se-Se chains is higher than that of S atoms, which prefer to bond with cation atoms [25, 73, 74, (ref. 46 in [74])]. Increasing of Δk_1 is accompanied by arising of new correlation characterizing the MRO of Ge–S. Therefore, we have three contributions for MRO, interchains Se-Se [75], interlayer structure of Ge-Se [66], and MRO of Ge–S. The difficulty arises because of the unresolved adjacent three contributions which overlap the positions. Evidence for this comes from the results of inelastic scattering of low energy neutrons [76], where the line associated with either edge-sharing tetrahedra or a vibrational mode of the Se-Se bonds on the edges of "outriggers rafts", is not resolved as a separate peak. Consequently, accruing of three types of MRO leads to broadening the FSDP. So, as we think, the results of Δk_1 cannot reflect a distortion on the MRO of our samples. The slight increase in both I_1 and k_1 could be explained according to the differences in the MRO amplitudes of Ge-Se and Ge–S. It is well-known that $f_S(k) < f_{Se}(k)$, then the growtgh of I_1 implies that MRO of this glasses not arise by correlations include S–S or S-Se atoms but arises by correlations containing Ge (Ge–S, and Ge-Se) [56]. We have explained above that the ability of S atoms to form bonds with Ge is higher than that of Se atoms. Then, we can consider that increasing in Ge–S correlations improve the MRO of our system which in turn increase the height I_1. This explanation is justified if we take into account the higher value of FSDP position of Ge–S system comparing with that of Ge-Se [42, 47], which explains the shift of k_1 of our glasses towards higher values.

3.2. Real-space properties

3.2.1. Short-range order of $Ge_{20}Se_{80-x}S_x$ glasses

The function $T(r)$ is normally used for extracting information regarding SRO [54]. The parameters describe SRO of glassy $Ge_{20}Se_{80-x}S_x$ samples such as the bond length and the coordination number can be extracted from the peak positions and the area under the peaks, respectively. Very high k-range is required to get high real-space resolution [78]. Shortness of the applied wavelength (0.1431 Å), combined with an appropriate data collection strategy was enabled to record data over a sufficiently high k-range. In these data k_{max} = 24 $\mathring{A}^{-1}$, which permits real space resolution limit of $\delta r = 2\pi/k_{max} = 0.26\mathring{A}$ [79].

Figure 2 shows $T(r)$ curves of our system. The curves show two strong peaks in r-range of $2.2\mathring{A} < r < 4.2\mathring{A}$. In general, $T(r)$ of $Ge_{20}Se_{80}$ glass is in a good agreement with previously published data [14, 15, 24, 80, 81]. It is easy to note some general behaviors at the first glance. With increasing S concentration from 0 to 30 at%, the first peak at $r \approx 2.36\mathring{A}$ shows slight shift to lower r-values with some decreasing in height and increasing in width. To understand these behaviors, we assigned in Fig. 3 the positions of Ge-Se, Se-Se, and Ge–S bonds, in crystalline $GeSe_2$, and GeS_2, respectively [82–84]. The structure of $Ge_{20}Se_{80}$ is

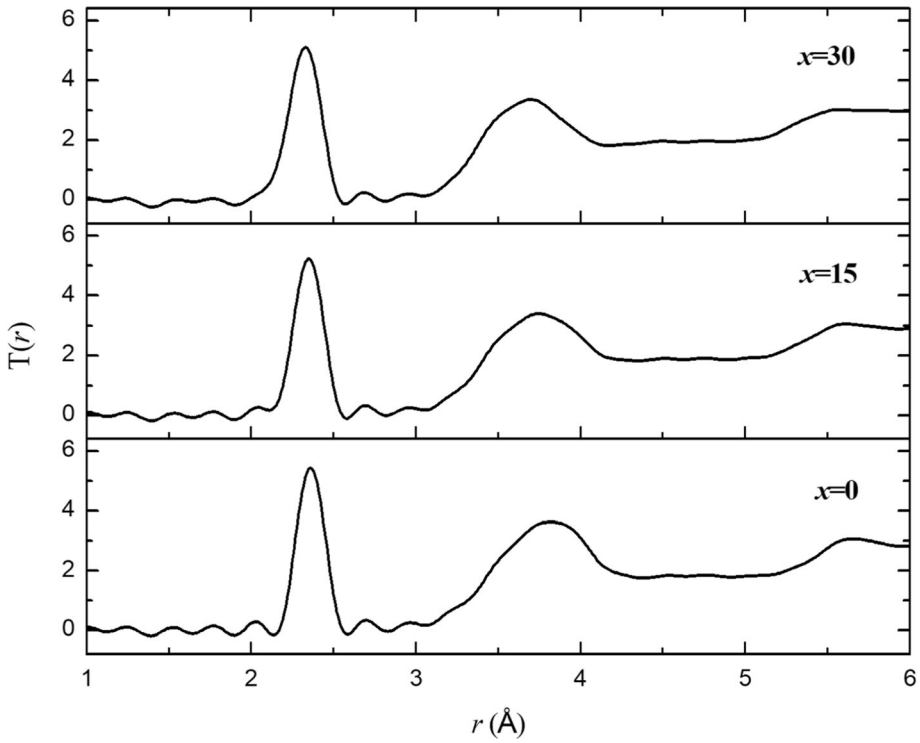

Fig. 2 Full-range plot of the total distribution function $T(r)$ of $Ge_xSe_{80-x}S_x$ glasses

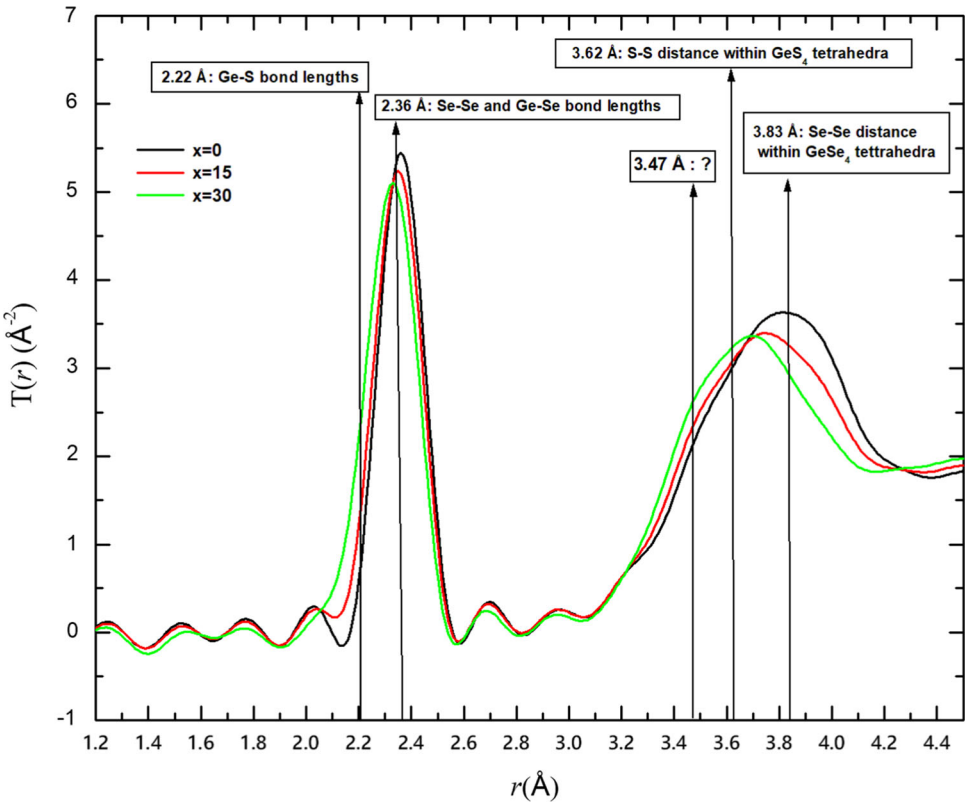

Fig. 3 The function $T(r)$ of $Ge_xSe_{80-x}S_x$ glasses. solid lines represent published bond lengths and interatomic distances. The correlations at 3.47 Å are ascribed to second neighbors of Ge atom as in Ge-Se-Se, or Ge-Se-S

frequently studied [14, 15, 24, 58, 74, 84–88]. The major attitude is that SRO consists of $GeSe_4$ tetrahedra connected through Se-Se bonds. This is evidently in Fig. 3. The position r_1 of the first peak at maximum-height coincidences with the length of Ge-Se and Se-Se bonds (2.36Å)[84]. This gives evidence that the first peak of $T(r)$

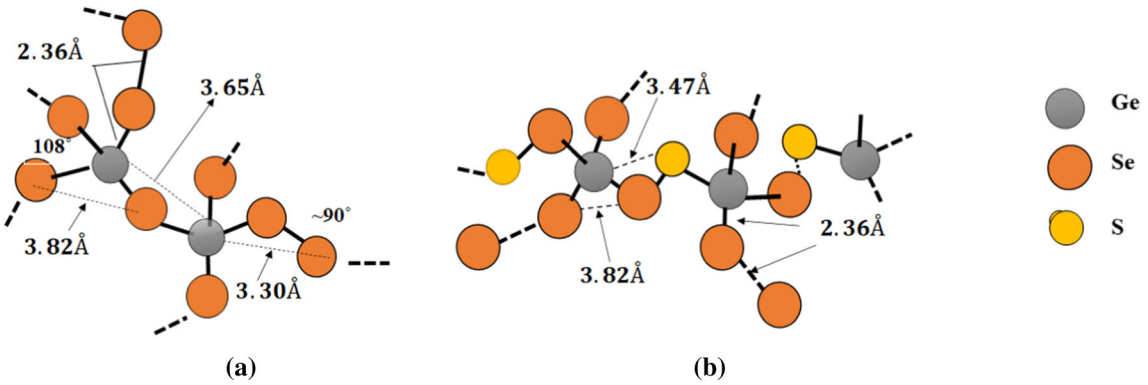

Fig. 4 Schematic representation of the atomic conformation in *g*lassy $Ge_{20}Se_{80-x}S_x$. **a** Stiffness composition (near $x = 0$). **b** Near x = 15

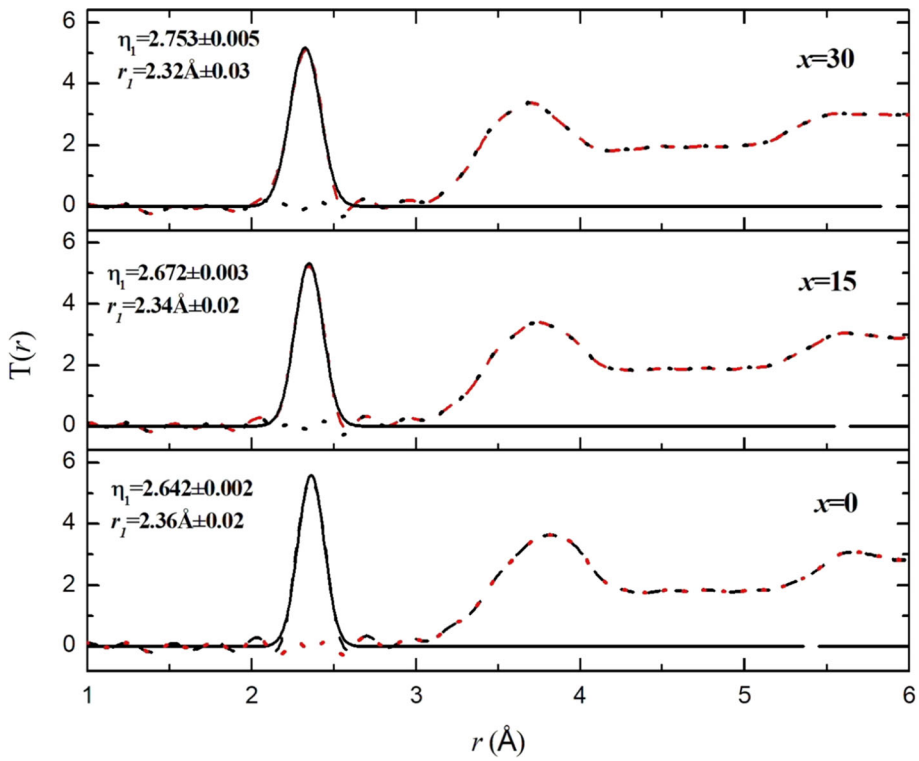

Fig. 5 Gaussian fitting of the first neighbor shell to the total correlation function, $T(r)$ for all the $Ge_{20}Se_{80-x}S_x$ alloys. Dashed line is $T(r)$; solid line is the fitted peaks and dotted-red line is the residual

curve in $Ge_{20}Se_{80}$ is basically governed by Ge-Se and Se-Se bonds. These two bonds contribute almost equally to the area of the first peak of $T(r)$ curve [84]. Increasing S-content at the expense of Se-content is accompanied by replacement of Se atoms at the corners of $GeSe_4$ tetrahedra by S atoms. Ge–S bond length (2.22Å) is shorter than both Ge-Se and Se-Se bonds [26, 83], which is the reason why the first peak shift to lower *r*- values with increasing S-content. The slight decrease in height and increase in width of the first peak with increasing S content may due to a small distortion in SRO with the small S percent incorporation within the lattice of Ge-Se glasses [90].

According to X-rays and neutrons diffraction data, $T(r)$ of the glassy system Ge_xSe_{100-x} $(x \geq 20\text{at}\%)$ shows small features (a weak peak or shoulder) at $r \approx 3.0-\ 3.3\text{Å}$. Anomalous x-ray scattering results show that the height of these features at $r = 3.3\text{Å}$ increases with decreasing x from $x = 0.23$ to $x = 0.195$ at% [30], while results of neutron diffraction show increasing the area of this peak on $T(r)$ curve with increasing x [14, 15]. These structures may be assigned to the correlation between a Ge atom at a tetrahedral center and a Se atom additionally attached to a tetrahedron corner, i.e., the Ge–(Se)–Se correlation [30]. Another viewpoint ascribes these features to Ge–Ge of edge-sharing $GeSe_4$ tetrahedra, like those in $Ge_{33}Se_{67}$ [14, 15, 24, 82, 92]. In fact, weakness of these features in addition to the spurious ripples, produced by the truncation the limited *k*-value, prevent a detailed discussion of the

atomic conformation in this range of distance [91]. Molecular dynamic modeling of liquid $Ge_{20}Se_{80}$, however, had shown that Ge–Ge correlation of corner- and edge-sharing spread out on a broad peak between 3 and 4 $\mathring{A}$ [24]. It is noteworthy that neutron diffraction study performed the absence of these features in S-enriched Ge–S system, with assertion to the existence of corner-sharing tetrahedra [93]. This may explains vanishing this shoulder with increasing S-content, look Fig. 3. At the same time, this vanishing is accompanied by strengthen a new one at$r \approx 3.47\mathring{A}$. The position of this structure is near the position $r = 3.47\mathring{A}$ previously observed in Ge–S and $Ge(Se_{1-x}S_x)_2$ [26, 83]. The origin of this structure is attributed to second neighbors of Ge atom as Ge-Se-Se, or Ge-Se-S in which highly crimped CS tetrahedra are connected through Se-Se or Se-S chains (look Fig. 3 in ref. [85] and Fig. 5 (d) in ref. [84]). The possibility of rocking Se-S(Se) bridging atoms causes changing the position between nearby $GeSe_4$ tetrahedra. This behavior was used to explain the abrupt increase in the mole polarization around the composition $Ge_{20}Se_{80}$ [94]. This effect in our case is accomplished by replacing some Se atoms with S atoms as shown, schematically, in Fig. 4.

The maximum height of the second peak is located at $r_{2_{max}} \approx 3.83\mathring{A}$, which is in a good agreement with the previously published data in case of $Ge_{20}Se_{80}$ [14, 15, 95]. This location corresponding to the Se-Se intratetrahedra distances. The bond angle θ $\left(\theta = 2\sin^{-1}(r_{2_{max}}/2r_1) = 108.47^{o}\right)$ are in a good agreement with the tetrahedral angle [17, 24, 64, 90]. With increasing S-content, this peak exhibits some shift towards lower *r*- values. This behavior is expected if we consider replacement Ge-Se bonds by Ge–S of shorter bond length, as we allowed before, see Fig. 4.

To examine SRO parameters, the first peak of $T(r)$was fitted using Gaussian function, [77]:

$$\boldsymbol{T(r) = a_1 \exp\left[-\left(\frac{r - r_1}{2u_1}\right)^2\right]} \quad (4)$$

where r_1 and u_1 represent, respectively, the position and the half-width at half-height of the first peak. The amplitude a_i is related to the area (the weighted average coordination number η_i) by:

$$\boldsymbol{a_1 = \frac{\eta_1}{2r_1u_1\sqrt{\pi}}} \quad (5)$$

Figure 5 shows the results of Gaussian fitting and SRO parameters**.** With S/Se replacement, the weighted coordination number η_1 vary slightly around an average value of 2.7. This refers to that S-atoms enter as compensations of Se atoms. It is well known that the SRO structure of $Ge_{20}Se_{80}$ can be well explained using chemical order network model CONM [24, 84]. Therefore, the comparable values of η_1 give us a semi-consensus that $Ge_{20}Se_{80-x}S_x$ glasses are governed by CONM [26, 30]. Investigation of this statement needs more assertion through calculating partial-structure factors and pair-correlation functions by using reverse Monte Carlo simulation and /or molecular dynamic simulation.

It is worth noting that, according to these results, replacing Se atoms with S-atoms transfers the structure of $Ge_{20}Se_{80-x}S_x$ from $Ge_{20}Se_{80}$ like-structure to $Ge_{20}S_{80}$ like-structure, and this is accompanied by increasing the ionic character of the compound [88]. This gradually transfers the applications of these materials to more ionic character-dependent properties.

4. Conclusions

High energy X-ray diffraction was applied to study the effect of S-atoms addition on both short-and medium-range order of $Ge_{20}Se_{80-x}S_x$ (where $x = 0$, 15 and 30 at%) chalcogenide glasses.. The origin of the first sharp diffraction peak on the structure factor was discussed according to the microcrystalline model. The results refer to increasing S-content leads to enhancement of the medium range order. Short-range order parameters indicate that S-atoms inter the host network of the stiffness composition $Ge_{20}Se_{80}$ as compensation of Se-atoms.

Author contribution AFE Data analysis and processing, Writing manuscript, discussion, preparing revised manuscript. MD supervision and discussion. MSE sample preparation, Data analysis and processing. SM Sample preparation.

Funding Openaccess funding provided by The Science, Technology & Innovation Funding Authority (STDF) incooperation with The Egyptian Knowledge Bank (EKB). This research work was funded by Science UP Faculty of Science grants, project number 6601. Therefore, authors gratefully acknowledge technical and financial support from the Academy of Science Research & Technology (**ASRT**).

Data availability The raw/processed data required to reproduce these findings cannot be shared at this time as the data also forms part of an ongoing study.

Declarations

Conflict of interest Authors declare that they have no conflict of interest.

References

[1] A F Abouraddy, M Bayindir, G Benoit, S D Hart, K Kuriki, N Orf, O Shapira, F Sorin, B Temelkuran and Y Fink *Nature Mater.* **6** 336 (2007)
[2] J Troles, F M Smektala, M Guignard, P Houizot, V Nazabal, H Zeghlache, G Boudebs, V Couderc Proc. 2005 7th Int. Conf. Transp. Opt. Netw. **2** p 242 (2005)
[3] S Kumar and M M Khan *Chalcogenide Lett.* **9** 145 (2012)
[4] N Mehta *Functional and Smart Materials* (eds) C Prakash, S Singh and J Paulo Davim (Boca Raton: CRC Press) Ch3, p 37(2020)
[5] N Mehta *Advances in Modern Sensors*; *Physics, design, simulation and applications* (eds) G R Sinha (Bristol UK: IOP eBooks, IOP Publishing) Ch4, p 4–1(2020)
[6] T Han, S Madden, D Bulla and B Luther-Davies *Optics Express* **18** 19286 (2010)
[7] M Kohl, A Kalendová, R Boidin and P Němec *Prog. Org. Coat.* **77** 1369 (2014)
[8] E L Gjersing, S Sen and B G Aitken *J. Phys. Chem. C* **114** 8601 (2010)
[9] M T Shatnawi, C L Farrow, P Chen, P Boolchand, A Sartbaeva, M F Thorpe and S J Billinge *Phys. Rev. B* **77** 094134 (2008)
[10] E Bychkov, C J Benmore and D L Price *Phys. Rev. B* **72** 172107 (2005)
[11] A H Moharram and A M Abdel-Baset *Phys. B Condens. Matter* **405** 4240 (2010)
[12] A Zeidler, J W Drewitt, P S Salmon, A C Barnes, W A Crichton, S Klotz, H E Fischer, C J Benmore, S Ramos and A C Hannon *J. Phys. Condens. Matter* **21** 474217 (2009)
[13] A Bytchkov, G J Cuello, S Kohara, C J Benmore, D L Price and E Bychkov *Phys. Chem. Chem. Phys.* **15** 8487 (2013)
[14] N R Rao, P S R Krishna, S Basu, B A Dasannacharya, K S Sangunni, E S R Gopal *J. Non-cryst. Solids 240* 221
[15] N R Rao, K S Sangunni, E S R Gopal, P S R Krishna, R Chakravarthy and B A Dasannacharya *Phys. B: Condens. Matter* **213** 561 (1995)
[16] O Uemura, T Usuki, A Murakami and Y Kameda *Phys. Status Solidi (a)* **170** 11 (1998)
[17] P S Salmon *J. Non-cryst. Solids* **353** 2959 (2007)
[18] R Azoulay, H Thibierge and A Brenac *J. Non-cryst. Solids* **18** 33 (1975)
[19] J C Phillips *J. Non-cryst. Solids* **34** 153 (1979)
[20] M F Thorpe *J. Non-cryst. Solids* **57** 355 (1983)
[21] U Senapati, K Firstenberg and A K Varshneya *J. Non-cryst. Solids* **222** 153 (1997)
[22] R Ota, T Yamate, N Soga and M Kunugi *J. Non-cryst. Solids* **29** 67 (1978)
[23] M Taniguchi, T Kouchi, L Ono, S Hosokawa, M Nakatake, H Namatame and K Murase *J. Elect. Spectrosc. Related Phenom.* **78** 507 (1996)
[24] M J Haye, C Massobrio, A Pasquarello, A De Vita, S W De Leeuw and R Car *Phys. Rev. B* **58** R14661 (1998)
[25] S R Elliott *Physics of Amorphous Materials* (Longman Group, Longman House, Burnt Mill, Harlow, Essex CM 20 2 JE, England) P66 (1983)
[26] Y Nagata, S Kokai, O Uemura and Y Kameda *J. Non-cryst. Solids* **169** 104 (1994)
[27] Y Wada, Y Wang, O Matsuda, K Inoue and K Murase *J. Non-cryst. Solids* **198** 732 (1996)
[28] H Xuecai, S Guangying, L Yu, Y Hongbo and L Yonghua *Chalcogenide Lett.* **9** 465 (2012)
[29] S Gu, N Zhang, Q Zhang and R Pan *Chalcogenide Lett.* **12** 257 (2015)
[30] M Dongol, A F Elhady, M S Ebied and A A Abuelwafa *Opt. Mater.* **78** 266 (2018)
[31] A P Hammersley, S O Svensson, M Hanfland, A N Fitch and D Hausermann *Int. J. High Pressure Res.* **14** 235 (1996)
[32] A P Hammersley, S O Svensson, M Hanfland, A N Fitch and D Häusermann *High Pressure Res.* **14** 235 (1996)
[33] Y Waseda *The Structure of Non-Crystalline Materials—Liquids and Amorphous Solids* (New York: McGraw-Hill) P28 (1980)
[34] J Krogh-Moe *Acta Crystallographica* **951**(1956)
[35] T E Faber and J M Ziman *Philosoph. Magaz.* **11** 153 (1965)
[36] P Juhás, T Davis, C L Farrow and S J Billinge *J. Appl. Crystallogr.* **46** 560 (2013)
[37] A Piarristeguy, M Mirandou, M Fontana and B Arcondo *J. Non-cryst. Solids* **273** 30 (2000)
[38] A Habenschuss and F H Spedding *J. Chem. Phys.* **70** 2806 (1979)
[39] G Lucovsky and J C Phillips *Nanoscale Res. Lett.* **5** 550 (2010)
[40] J M Zaug, A K Soper and S M Clark *Nature Mater.* **7** 890 (2008)
[41] J C Phillips *J. Non-cryst. Solids* **43** 37 (1981)
[42] K Tanaka *Japanese J. Appl. Phys.* **37** 1747 (1998)
[43] L E Busse *Phys. Rev. B* **29** 3639 (1984)
[44] S Susman, D L Price, K J Volin, R J Dejus and D G Montague *J. Non-cryst. Solids* **106** 26 (1988)
[45] L Červinka *J. Non-cryst. Solids* **106** 291 (1988)
[46] S R Elliott *J. Phys. Condensed Matter* **4** 7661 (1992)
[47] S C Moss and D L Price *Phys. Disordered Mater.* (Boston: Springer) P77 (1985)
[48] R Golovchak, P Lucas, J Oelgoetz, A Kovalskiy, J York-Winegar, C Saiyasombat, O Shpotyuk, M Feygenson, J Neuefeind and H Jain *Mater. Chem. Phys.* **153** 432 (2015)
[49] P Debye *Ann. Phys* **46** 21 (1915)
[50] A H Compton and S K Allison *X-rays in Theory and Experiment* (New York : D. VAN NOSTRAND COMPANY, INC.) P 134 (1935)
[51] G Breitlingand and H Richter *Mater. Res. Bull.* **4** 19 (1969)
[52] L Červinka *J. Non-cryst. Solids* **232** 1 (1998)
[53] S R Elliott *J. Non-cryst. Solids* **182** 40 (1995)
[54] A C Wright, R A Hulme, D I Grimley, R N Sinclair, S W Martin, D L Price and F L Galeener *J. Non-cryst. Solids* **129** 213 (1991)
[55] S Mamedov, A Bolotov, L Brinker, A Kisliuk, M Soltwisch, M Vlcek and A Sklenar *Phys. Rev. B* **58** 8155 (1998)
[56] O Uemura, T Usuki, A Murakami and Y Kameda *Phys. Statussolidi (a)* **170** 11 (1998)
[57] P S Salmon, R A Martin, P E Mason and G J Cuello *Nature* **435** 75 (2005)
[58] M Bauchy, M Micoulaut, M Boero and C Massobrio *Phys. Rev. Lett.* **110** 165501 (2013)
[59] S Hosokawa *J. Optoelectron. Adv. Mater.* **3** 199 (2001)
[60] D A Drabold *Phys. Rev. B* **71** 054206 (2005)
[61] L Fan, D Paterson, I McNulty, M M J Treacy and J M Gibson *J. Microsc.* **225** 41 (2007)
[62] S R Elliott *Nature* **354** 445 (1991)

[63] P M Bridenbaugh, G P Espinosa, J E Griffiths, J C Phillips and J P Remeika *Phys.Rev. B* **20** 4140 (1979)
[64] Y Murakami, T Usuki, M Sakurai, S Kohara, *Mater. Sci. Eng. A* **449** (2007)
[65] P Vashishta, R K Kalia and I Ebbsjö *Phys. Rev. B* **39** 6034 (1989)
[66] Y Wang, E Ohata, S Hosokawa, M Sakurai and E Matsubara *J. Non-cryst. Solids* **337** 54 (2004)
[67] K D Machado, J C De Lima, C E M Campos, A A M Gasperini, S M De Souza, C E Maurmann, T A Grandi and P S Pizani *Solid State Commun.* **133** 411 (2005)
[68] R J Nemanich, S A Solin and G Lucovsky *Solid State Commun.* **21** 273 (1977)
[69] P M Bridenbaugh, G P Espinosa, J E Griffiths, J C Phillips and J P Remeika *Phys. Rev. B* 4140 (1979)
[70] G Dittmar and H Schäfer *Chemistry* **31** 2060 (1975)
[71] A Bouzid, S Le Roux, G Ori, M Boero and C Massobrio *J. Chem. Phys.* **143** 034504 (2015)
[72] W Li, S Seal, C Rivero, C Lopez, K Richardson, A Pope, A Schulte, S Myneni, H Jain, K Antoine and A C Miller *J. Appl. Phys.* **98** 053503 (2005)
[73] W Li, S Seal, C Rivero, C Lopez and K A Richardson *J. Appl. Phys.* **92** 7102 (2002)
[74] J C Malaurent and J Dixmier *J. Non-cryst. Solids* **35** 1227 (1980)
[75] K Tanaka *Phys. Rev. B* **39** 1270 (1989)
[76] L F Gladden, S R Elliott, R N Sinclair and A C Wright *J. Non-cryst. Solids* **106** 120 (1988)
[77] M Dongol, T Gerber, M Hafiz, M Abou-Zied and A F Elhady *J. Phys. Condens. Matter* **18** 6213 (2006)
[78] V Petkov, I K Jeong, J S Chung, M F Thorpe, S Kycia and S J Billinge *Phys. Rev. Lett.* **83** 4089 (1999)
[79] B Himmel, J Claudius, T Gerber and C Reinhold *J. Non-cryst. Solids* **162** 136 (1993)
[80] M T Shatnawi *New J. Glass Ceram.* **5** 31 (2015)
[81] M Micoulaut, A Kachmar, M Bauchy, S Le Roux, C Massobrio and M Boero *Phys. Rev. B* **88** 054203 (2013)
[82] I Petri and P S Salmon *Phys. Chem. Glasses* **43** 185 (2002)
[83] Y Sakaguchi, T Hanashima, K Ohara, A A A Simon and M Mitkov *Phys. Rev. Mater.* **3** 035601 (2019)
[84] B Kalkan, R P Dias, C S Yoo, S M Clark and S Sen *J. Phys. Chem. C* **118** 5110 (2014)
[85] P Tronc, M Bensoussan, A Brenac and C Sebenne *Phys. Rev. B* **8** 5947 (1973)
[86] P Tronc, M Bensoussan, A Brenac and C Sebenne *Solid State Commun.* **24** 79 (1977)
[87] P Tronc *J. de Phys.* **51** 675 (1990)
[88] A Bouzid, K J Pizzey, A Zeidler, G Ori, M Boero, C Massobrio, S Klotz, H E Fischer, C L Bull and P S Salmon *Phys. Rev. B* **93** 014202 (2016)
[89] O Uemura, T Satow and Y Sagara *Phys. Status Solidi a* **32** K91 (1975)
[90] G Dittmar and H Schäfer *Chemistry* **32** 118 (1976)
[91] S Hosokawa, L Oh, M Sakurai, W C Pilgrim, N Boudet, J E Bérar and S Kohara *Phys. Rev. B* **84**, no. 1 (2011)
[92] S Susman, K J Volin, D G Montague and D L Price *J. Non-cryst. Solids* **125** 168 (1990)
[93] A Banez, M Bionducci, E Philippot, L Descôtes and R Bellissent *J. Non-cryst. Solids* **202** 248 (1996)
[94] A Feltz, H Aust and A Blayer *J. Non-cryst. Solids* **55** 179 (1983)
[95] C Massobrio, M Celino, P S Salmon, R A Martin, M Micoulaut and A Pasquarello *Phys. Rev. B* **79** 174201 (2009)